Channel Modeling of RIS-Assisted Vehicular Communications With Delayed Reconfiguration

Asad Saleem
School of Electronic Engineering and Intelligent Manufacturing, Anhui Xinhua University, Hefei, 230088, China
asadalvi64@yahoo.com

Mohammad Jafar Mokarram
School of Electronic Engineering and Intelligent Manufacturing, Anhui Xinhua University, Hefei, 230088, China
mjmokarram@axhu.edu.cn

Sun Meiling*
School of Electronic Engineering and Intelligent Manufacturing, Anhui Xinhua University, Hefei, 230088, China
sunmeiling3902@163.com

Shizhao Huang
School of Electronic Engineering and Intelligent Manufacturing, Anhui Xinhua University, Hefei, 230088, China
huangshizhao@axhu.edu.cn

Temitope E. Komolafe
Collaborative Research Center, Shanghai University of Medicine & Health Sciences, Shanghai, 201318, China
teakomo@mail.ustc.edu.cn

Yan Xu
School of Opto-Electronics Engineering , Zaozhuang University, Zaozhuang 277160 , China
zzuxuy@163.com

***Abstract*—Reconfigurable intelligent surfaces (RISs) can enhance vehicular wireless links at millimeter-wave frequencies, where mobility leads to rapid channel variation. With finite update intervals, however, the RIS phase profile becomes outdated, causing phase mismatch and loss of coherent combining gain. This paper develops a three-dimensional geometry-based stochastic model (3D-GBSM) for RIS-assisted vehicular channels under delayed reconfiguration. The model relates vehicle motion and RIS update intervals to phase mismatch and the resulting channel response. The effects of update interval and vehicle speed on received signal-to-noise ratio (SNR) and reliability are evaluated under different mobility conditions. The analysis establishes the maximum allowable RIS update interval and a phase-error-limited interval, while achievable-rate results are compared with existing RIS-assisted vehicular studies. Results show that increasing mobility accelerates channel aging and requires more frequent RIS reconfiguration.**

***Index Terms*—Reconfigurable intelligent surface (RIS); 3D-GBSM channel modeling; channel aging; finite update interval**

I. Introduction

Vehicle-to-Everything (V2X) communication combines Vehicle-to-Vehicle (V2V) and Vehicle-to-Infrastructure (V2I) links to support intelligent transportation, cooperative driving, and autonomous mobility, where reliable low-latency connectivity must be maintained under rapidly changing propagation conditions [1]. Millimeter-wave (mmWave) communication offers the bandwidth required for data-intensive vehicular applications, although blockage, beam misalignment, Doppler effects, and mobility-driven non-stationarity can substantially affect mmWave channels [2]. Geometry-based stochastic model (GBSM) provides a tractable framework for representing mobility, path evolution, and phase variation [3], while 3D-GBSM captures spatiotemporal channel behavior through cluster- and ray-based components.

Reconfigurable intelligent surfaces (RISs), also known as intelligent reflecting surfaces (IRSs), can improve vehicular coverage through controllable reflected paths that mitigate blockage with low hardware power consumption [4]. RIS-assisted vehicular research has primarily addressed channel estimation, beam control, and mobility-aware adaptation [4], but has not quantified how finite update intervals affect reflected-path phase alignment during vehicle motion. The non-stationary RIS-assisted V2V model in [5] characterized the geometric evolution of vehicular channels, but assumed timely RIS adaptation without considering delayed reconfiguration or outdated phase profiles. Studies of outdated channel state information (CSI) have shown that mobility can rapidly invalidate estimated RIS channels [6], while experiments have identified feedback and beam-tracking latency as practical limitations [7]. Nevertheless, existing studies do not provide a geometry-based vehicular channel model that explicitly links vehicle motion and RIS update interval to reflected-path phase mismatch and subsequent SNR, achievable rate, and reliability, together with a practical update-timing criterion.

To address this gap, this paper develops a 3D-GBSM for RIS-assisted vehicular communication under delayed reconfiguration. The model separates the ideal RIS phase profile from the outdated profile retained during each update interval and links mobility-induced phase mismatch to cascaded propagation-distance variations. The effects of delayed updating on received SNR and reliability are evaluated under different mobility conditions and RIS sizes. The analysis determines the maximum allowable RIS update interval and derives a phase-error-limited interval for mobility-dependent RIS control. Achievable-rate results are compared with existing literature to assess consistency.

II. System Model and Formulation

A. Vehicular RIS Channel With Delayed Reconfiguration

Consider a roadside RIS-assisted V2V link at carrier frequency f_c, where $\lambda = c/f_c$. The RIS contains $M = M_x \times M_y$ passive elements in a uniform planar array. Fig. 1 illustrates the system geometry and representative 3D clustered scattering

979-8-3195-0167-7/26/$31.00 ©2026 IEEE

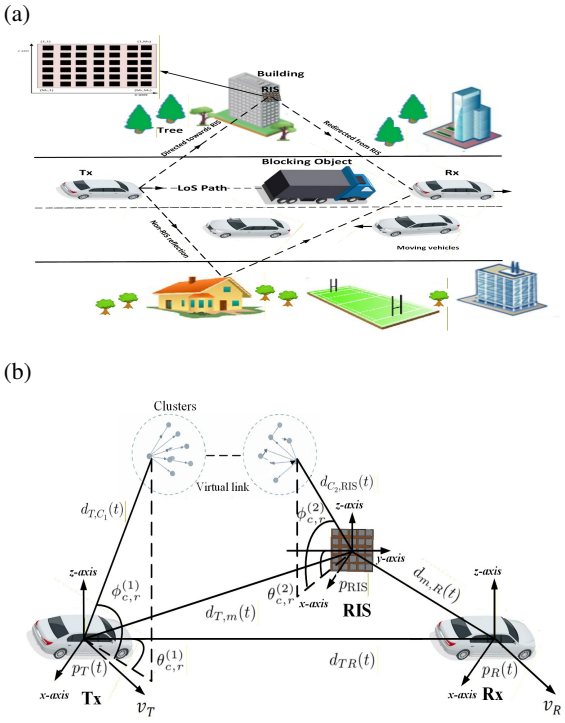


Fig. 1. Proposed RIS-assisted vehicular communication geometry for delayed RIS reconfiguration. (a) Overall system model, (b) Representative clustered scattering geometry for Tx–RIS subchannel with azimuth and elevation angles.

structure. Let $p_T(t)$, $p_R(t)$, and p_{RIS} denote the Tx, Rx, and RIS-center positions. The m-th RIS element is defined as [3]

$$p_m = p_{RIS} + \begin{bmatrix} \left(m_x - \dfrac{M_x+1}{2}\right) d_x \\ \left(m_y - \dfrac{M_y+1}{2}\right) d_y \\ 0 \end{bmatrix} \tag{1}$$

where d_x and d_y are the inter-element spacings, with $m_x = 1,\ldots,M_x$ and $m_y = 1,\ldots,M_y$. The corresponding link distances are

$$\begin{aligned} d_{T,m}(t) &= |p_T(t) - p_m|,\ d_{m,R}(t) = |p_m - p_R(t)|, \\ d_{TR}(t) &= |p_T(t) - p_R(t)| \end{aligned} \tag{2}$$

For propagation distance d, $L_{fs}(d) = \left(\frac{\lambda}{4\pi d}\right)^2$. The RIS reflection matrix is

$$\Theta(t) = \mathrm{diag}\left(\beta_1 e^{j\varphi_1(t)}, \beta_2 e^{j\varphi_2(t)}, \ldots, \beta_M e^{j\varphi_M(t)}\right) \tag{3}$$

where $\beta_m \in [0,1]$ and $\varphi_m(t) \in [0, 2\pi)$ represent the reflection amplitude and phase shift of the m-th element, respectively. With $u(\theta,\phi) = [\cos\phi\cos\theta, \cos\phi\sin\theta, \sin\phi]^T$ denoting the 3D unit propagation vector for azimuth θ and elevation ϕ, the Tx–RIS and RIS–Rx links follow the same cluster-ray formulation:

$$h_{i,m}(t) = \sqrt{L_{fs}(d_{i,m}(t))}\,\alpha_{i,m}(t) e^{-j\frac{2\pi}{\lambda} d_{i,m}(t)}, \qquad i \in \{1,2\} \tag{4}$$

where $d_{1,m}(t) = d_{T,m}(t)$ and $d_{2,m}(t) = d_{m,R}(t)$. The small-scale coefficient is

$$\begin{aligned} \alpha_{i,m}(t) = \sum_{c=1}^{C_i}\sum_{r=1}^{R_c} a_{c,r}^{(i)} e^{j\left(2\pi f_{D,c,r}^{(i)}(t) t + \phi_{c,r}^{(i)}\right)} \\ \times e^{-j\frac{2\pi}{\lambda} u^T\left(\theta_{c,r}^{(i)}, \varphi_{c,r}^{(i)}\right)(p_m - p_{RIS})} \end{aligned} \tag{5}$$

where C_i, R_c, $a_{c,r}^{(i)}$, $\theta_{c,r}^{(i)}$, $\varphi_{c,r}^{(i)}$, and $f_{D,c,r}^{(i)}(t)$ represent the number of clusters, rays per cluster, amplitude, azimuth, elevation, and Doppler shift, respectively. The direct Tx–Rx subchannel is

$$\begin{aligned} h_3(t) = \sqrt{L_{fs}(d_{TR}(t))} \sum_{c=1}^{C_3}\sum_{r=1}^{R_c} a_{c,r}^{(3)} \\ \times e^{j\left(2\pi f_{D,c,r}^{(3)}(t) t + \phi_{c,r}^{(3)}\right)} e^{-j\frac{2\pi}{\lambda} d_{TR}(t)} \end{aligned} \tag{6}$$

where C_3 is the number of direct-link clusters. No RIS spatial phase term is included in the direct Tx–Rx link [8]. Let $h_1(t) = [h_{1,1}(t),\ldots,h_{1,M}(t)]^T$ and $h_2(t) = [h_{2,1}(t),\ldots,h_{2,M}(t)]^T$ denote the Tx–RIS and RIS–Rx subchannel vectors, respectively. The effective RIS-assisted channel is

$$h_{\text{eff}}(t) = h_3(t) + h_2^H(t)\Theta(t)h_1(t) \tag{7}$$

where $(\cdot)^H$ denotes Hermitian transpose. Ideal phase compensation uses

$$\phi_m^*(t) = \frac{2\pi}{\lambda}\left[d_{T,m}(t) + d_{m,R}(t)\right] \tag{8}$$

which aligns the cascaded path. The corresponding SNR and rate are

$$\gamma(t) = \frac{P_t |h_{\text{eff}}(t)|^2}{N_0}, \qquad R(t) = \log_2(1+\gamma(t)) \tag{9}$$

where P_t and N_0 are the transmit and noise powers. Practical control introduces finite RIS update delays.

B. Delayed RIS Reconfiguration and Channel Aging Model

To model finite RIS controller response, the RIS is updated at discrete instants $t_u = kT_u$, where T_u is the update interval and $k \in \mathbb{Z}_{\geq 0}$. The phase profile therefore remains fixed within each update block:

$$\Theta(t) = \Theta(t_u), \qquad t_u \leq t < t_u + T_u \tag{10}$$

At t_u, the RIS phase is set using the corresponding cascaded Tx–RIS–Rx distances. Vehicle motion changes these distances, making the applied phase outdated. The resulting phase mismatch is

$$\Delta\phi_m(t) = \frac{2\pi}{\lambda}\left[d_{T,m}(t) + d_{m,R}(t) - d_{T,m}(t_u) - d_{m,R}(t_u)\right] \tag{11}$$

Under delayed reconfiguration, the effective channel becomes

$$h_{\text{eff}}^{(a)}(t) = h_3(t) + h_2^H(t)\Theta(t_u)h_1(t) \tag{12}$$

where the superscript (a) denotes the aged channel under delayed RIS control. The delayed phase profile reduces coherent combining as the channel evolves. To capture mobility in the

TABLE I
SIMULATION PARAMETERS

Parameter	Value
Carrier frequency, f_c	28 GHz
Transmit power, P_t	20 dBm
Noise power, N_0	-94 dBm
Tx initial position, $p_T(0)$	(0, 0, 1.5) m
Rx initial position, $p_R(0)$	(40, 0, 1.5) m
RIS center position, p_{RIS}	(20, 6, 6) m
RIS element spacing	$\lambda/2$
Vehicle speed	20–120 km/h
RIS update interval, T_u	1–50 ms
Reflection amplitude, β_m	1
SNR threshold, γ_{th}	5 dB

3D-GBSM, the Doppler shift of the r-th ray in the c-th cluster for link i is [5]

$$f_{D,c,r}^{(i)}(t) = \frac{1}{\lambda} v_i^T(t) u\left(\theta_{c,r}^{(i)}, \phi_{c,r}^{(i)}\right), \quad i \in \{1,2,3\} \tag{13}$$

where $v_i(t)$ denotes the relative velocity vector and $u(\theta_{c,r}^{(i)}, \phi_{c,r}^{(i)})$ the 3D propagation direction. Higher mobility increases Doppler shifts and accelerates RIS phase misalignment. The aged SNR and achievable rate are

$$\gamma^{(a)}(t) = \frac{P_t |h_{\mathrm{eff}}^{(a)}(t)|^2}{N_0}, \qquad R^{(a)}(t) = \log_2\left(1 + \gamma^{(a)}(t)\right) \tag{14}$$

The reliability probability over the random cluster-ray realizations is defined as

$$P_{\mathrm{rel}}(T_u) = \Pr\left(\gamma^{(a)}(t) \geq \gamma_{\mathrm{th}}\right) \tag{15}$$

where γ_{th} is the minimum required SNR. The maximum admissible RIS update interval satisfying a reliability target P_0 is

$$T_u^* = \max\left\{T_u : \; P_{\mathrm{rel}}(T_u) \geq P_0\right\} \tag{16}$$

For small elapsed time after the latest RIS update, a first-order expansion of the phase mismatch around $t = t_u$ gives

$$\Delta\phi_m(t) \approx \frac{2\pi}{\lambda}\left[\dot{d}_{T,m}(t_u) + \dot{d}_{m,R}(t_u)\right](t - t_u) \tag{17}$$

Thus, imposing $|\Delta\phi_m(t)| \leq \phi_{\max}$ yields a mobility-dependent update constraint. Averaging over all RIS elements gives

$$\bar{T}_u^{(\phi)} = \frac{1}{M}\sum_{m=1}^{M} \frac{\phi_{\max}\lambda}{2\pi\left|\dot{d}_{T,m}(t_u) + \dot{d}_{m,R}(t_u)\right|} \tag{18}$$

Higher geometric variation rates require shorter RIS update intervals, complementing the reliability-based criterion in (16).

III. Simulation Setup and Numerical Results

A. Simulation Setup

Numerical simulations consider a roadside mmWave V2V scenario with $f_c = 28$ GHz. The initial positions are $p_T(0) = (0, 0, 1.5)$ m, $p_R(0) = (40, 0, 1.5)$ m, and $p_{\mathrm{RIS}} = (20, 6, 6)$ m, with $P_t = 20$ dBm and $N_0 = -94$ dBm. The RIS employs an 8×8 array with $d_x = d_y = \lambda/2$ and $\beta_m = 1$. Cluster visibility evolves with vehicle motion following the birth-death process in [9], with $R_c = 10$ rays per cluster. For each vehicle speed and RIS update interval, $N_t = 100$ time samples and 1000 independent Monte Carlo realizations are evaluated to obtain the aged SNR, reliability, and phase-error-limited update interval. Table I summarizes the default parameters.

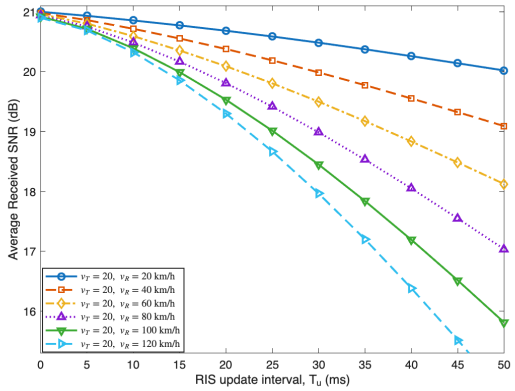


Fig. 2. Received SNR versus RIS update interval for different same-direction mobility conditions, with fixed $v_T = 20$ km/h and $M = 64$.

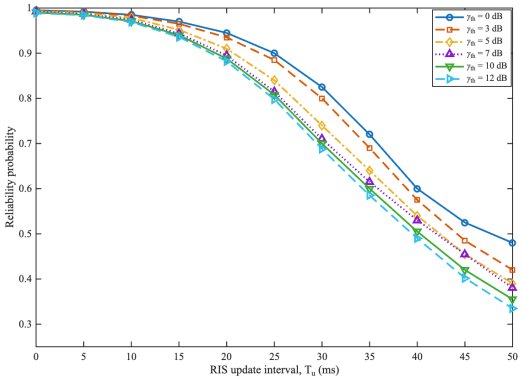


Fig. 3. Reliability versus RIS update interval for different SNR thresholds at $v_T = 40$ km/h and $v_R = 80$ km/h.

B. Results and Discussion

Fig. 2 presents the average received SNR versus RIS update interval under same-direction mobility. As the interval increases, the outdated RIS phase profile weakens coherent combining and reduces SNR. This loss is more pronounced at higher Rx speeds, where faster geometric variation causes quicker phase misalignment, consistent with [6].

Fig. 3 presents reliability versus RIS update interval for different SNR thresholds. Reliability decreases with T_u as accumulated phase mismatch lowers the aged SNR, with higher thresholds producing lower reliability. Stricter reliability requirements therefore require shorter RIS update intervals.

Fig. 4 presents the maximum allowable RIS update interval T_u^* versus vehicle speed for different RIS sizes. T_u^* decreases with speed as faster channel aging makes the RIS phase

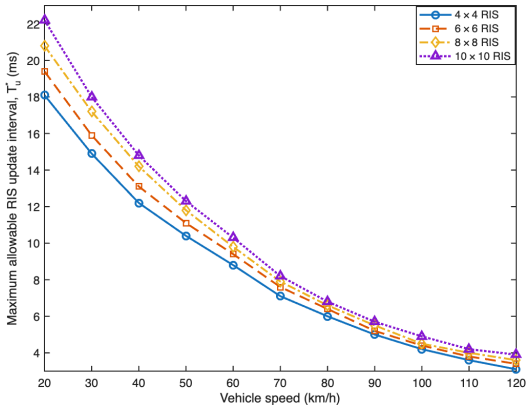


Fig. 4. Maximum allowable RIS update interval T_u^* versus vehicle speed for different RIS sizes under delayed RIS reconfiguration.

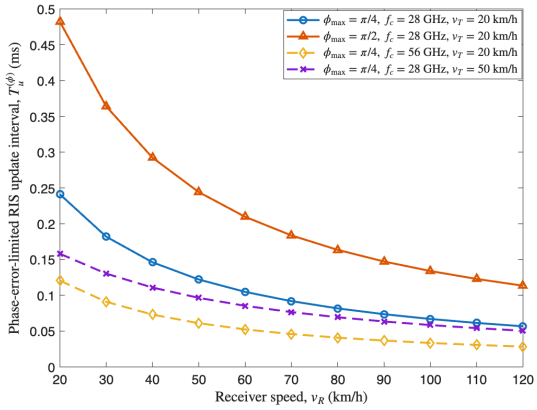


Fig. 5. Phase-error-limited RIS update interval versus receiver speed for different phase-error thresholds, carrier frequencies, and transmitter speeds.

profile outdated sooner. Larger arrays allow slightly longer intervals through stronger reflected-path gain, although this benefit diminishes at higher speeds.

Fig. 5 presents the analytical phase-error-limited RIS update interval. The interval decreases with v_R, while $\phi_{\max} = \pi/2$ allows longer intervals than $\phi_{\max} = \pi/4$. Higher carrier frequency and v_T further shorten the interval by accelerating phase variation. These trends agree with the reliability-based results in Fig. 4.

Fig. 6 presents the achievable rate versus transmit power for different RIS sizes. Both RIS-assisted cases outperform the without-RIS case, with the 16×16 RIS achieving the highest rate through stronger reflected-link gain. The similar trend in [10] provides a qualitative consistency check of the proposed model.

IV. Conclusion

This paper developed a 3D-GBSM for RIS-assisted vehicular communications under delayed reconfiguration. Longer update intervals increase phase mismatch and degrade SNR, rate, and reliability, particularly at higher speeds. The reliability-

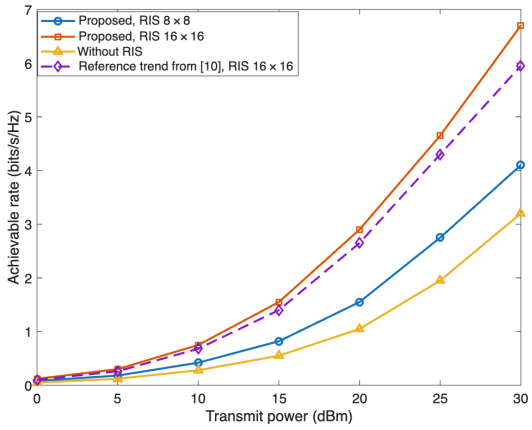


Fig. 6. Achievable rate versus transmit power for different IRS sizes and the 16×16 IRS reference in [10].

and phase-error-based criteria show that higher mobility and carrier frequency require more frequent RIS updates. Therefore, RIS-assisted vehicular systems should adapt update frequency to mobility, RIS size, and performance requirements.

Acknowledgment

This work was supported by the National Natural Science Foundation of China (W2433153), Anhui Provincial Department of Education Natural Science Research Project (2025AHGXZK31529), and Anhui Xinhua University Research Start-Up Fund for Young Doctoral Research (2026kyqd18).

References

[1] Y. Huang and Y. Zhao, "Beam management for millimeter-wave mobile communications based on digital twin-enabled scenario cognition," *Sci. Rep.*, vol. 15, Art. no. 13802, Apr. 2025.

[2] J. Qian *et al.*, "Path loss model for 3.5 GHz and 5.6 GHz bands in cascaded tunnel environments," *Sensors*, vol. 22, no. 12, p. 4524, Jun. 2022.

[3] A. Saleem and S. Tan, "Modeling of intelligent reflecting surface based 3-D non-stationary massive MIMO channel for vehicle-to-vehicle communications," *Electromagn. Sci.*, vol. 3, no. 4, Art. no. 0120382, pp. 0120382-1–0120382-20, Dec. 2025.

[4] M. Deng *et al.*, "Reconfigurable intelligent surfaces enabled vehicular communications: A comprehensive survey of recent advances and future challenges," *IEEE Trans. Intell. Veh.*, vol. 10, no. 8, pp. 4191–4216, Aug. 2025.

[5] W. Shi *et al.*, "RIS-empowered V2V communications: Three-dimensional beam domain channel modeling and analysis," *IEEE Trans. Wireless Commun.*, vol. 23, no. 11, pp. 15844–15857, Nov. 2024.

[6] S. Deb and S. C. Ghosh, "Time varying channel estimation for RIS assisted network with outdated CSI: Looking beyond coherence time," *Comput. Commun.*, vol. 240, Art. no. 108202, Aug. 2025.

[7] Z. Wang and Y. Nie, "Experimental studies on low-latency RIS beam tracking: Edge-integrated and visually steered," *Network*, vol. 5, no. 3, Art. no. 22, Jul. 2025.

[8] A. Saleem *et al.*, "A non-stationary 3D-GBSM V2V channel model for wideband massive MIMO systems," *IEEE Commun. Lett.*, vol. 27, no. 1, pp. 19-23, Jan. 2023.

[9] A. Saleem *et al.*, "Statistical characteristics of 3D MIMO channel model for vehicle-to-vehicle communications," *Wirel. Commun. Mob. Comput.*, vol. 2022, no. 1, p. 9090494, Jun. 2022.

[10] D. Dampahalage *et al.*, "Intelligent reflecting surface aided vehicular communications," in *Proc.IEEE Globecom Workshops (GC Wkshps)*, Taipei, Taiwan, 2020, pp. 1-6,